# Impact of thermal strain on the dielectric constant of sputtered barium strontium titanate thin films

T. R. Taylor and P. J. Hansen
*Materials Department, College of Engineering, University of California, Santa Barbara, California 93106*

B. Acikel, N. Pervez, and R. A. York
*Department of Electrical and Computer Engineering, College of Engineering, University of California, Santa Barbara, California 93106*

S. K. Streiffer
*Materials Science Division, Argonne National Laboratory, Argonne, Illinois 60439-4838*

J. S. Speck[a)]
*Materials Department, College of Engineering, University of California, Santa Barbara, California 93106*

(Received 6 November 2001; accepted for publication 10 January 2002)

Barium strontium titanate thin films were deposited by sputtering on Pt/$SiO_2$ structures using five different host substrates: magnesium oxide, strontium titanate, sapphire, silicon, and vycor glass. These substrates were chosen to provide a systematic change in thermal strain while maintaining the same film microstructure. All films have a weakly textured microstructure. Temperature dependent dielectric measurements from 100–500 K determined that decreasing thermal expansion coefficient of the host substrate (i.e., larger tensile thermal strain) reduced the film dielectric permittivity. The experimentally determined Curie–Weiss temperature decreased with increasing tensile thermal strain and the Curie–Weiss constant increased with tensile strain as predicted by Pertsev *et al.* [J. Appl. Phys. **85**, 1698 (1999)]. © *2002 American Institute of Physics.* [DOI: 10.1063/1.1459482]

Oxide thin films remain very attractive to researchers due to their wide range of useful physical properties. Most groups have focused on the fabrication of thin films for optical and dielectric applications. The properties of oxide/ferroelectric thin films deviate from their bulk counterparts. Specifically, the (Ba,Sr)$TiO_3$ (BST) and Pb(Zr,Ti)$O_3$ systems display a range of size dependent properties. A large amount of literature has emerged on the epitaxial growth of ferroelectric thin films and subsequent stress relaxation.[1–4] The properties of polycrystalline ferroelectric thin films grown on metal electrodes are more difficult to understand mainly due to the oxide film electrode interface and nanocrystalline microstructure. Grain size suppression, interfacial chemical reactions, and the exact nature of the metal–oxide contact are poorly understood. Strain also has a major influence on film properties.[5] In epitaxial film systems, it has been proposed that the misfit strain between the film and substrate can suppress the stable ferroelectric phase.[5] When the paraelectric phase is placed under biaxial tension due to the substrate, a contraction occurs along the film normal, *c* axis, resulting in an in-plane orientation of the polar axis.[5,6]

In this letter, the impact of thermal strain on the film dielectric constant was investigated. Films were deposited concurrently by rf magnetron sputtering on Pt/$SiO_2$ using five different support substrates: magnesium oxide, sapphire, silicon, strontium titanate, and vycor glass. The growth chamber has sputtering sources 30° off axis from the heated substrate with a 4.25 in. source to substrate distance. To avoid texture variation between films resulting from different substrates and growth surfaces, each substrate had 60 nm of $SiO_2$ deposited by plasma-enhanced chemical vapor deposition at 250 °C. The samples were radially loaded onto the substrate holder after being ultrasonically cleaned in acetone, followed by isoproponal, and baked at 115 °C for 10 min. Prior to film growth, the $SiO_2$ layer was heat treated in 25 mTorr of oxygen at 750 °C for 30 min. Subsequently, a 100 nm platinum bottom electrode was grown. Approximately 5 nm of Zr was used as an adhesion layer between the $SiO_2$ and Pt. X-ray diffraction (XRD) measurements revealed (111) textured polycrystalline platinized substrates with (111) Pt rocking curves full width at half maximum values from 5°–7°. Additional platinized substrates were characterized by atomic force microscopy (AFM) to insure that the Pt growth surfaces were similar across the samples. Stoichiometric $Ba_{0.3}Sr_{0.7}TiO_3$ targets were used to deposit the 100 nm BST film. Separate samples grown for AFM and XRD measurements showed polycrystalline films with weak (100) and (110) texture and similar surface morphology. The AFM images and XRD data revealed no distinguishing features between the samples. The (111) BST peak can not be detected because of the overlap with the (111) Pt peak. The BST film composition was determined from a separate standard by Rutherford backscattering spectroscopy (RBS) yielding a (Ba+Sr)/Ti and Ba/Sr ratio of approximately 1.04 and 0.32, respectively ($Ba_{0.24}Sr_{0.76}Ti_{0.96}O_3$). The specific growth conditions for the Zr, Pt, and BST films are given in Table I.

Parallel plate capacitors were fabricated on the BST/Pt/substrate samples by a two-step mask process. The first mask level was an HF etch mask that was used to isolate and define the active dielectric area. The second mask step defined the top electrode area by a liftoff method. Pt (100 nm)/Au (100 nm) top contacts were deposited by electron-

[a)]Electronic mail: speck@mrl.ucsb.edu

0003-6951/2002/80(11)/1978/3/$19.00

© 2002 American Institute of Physics
Downloaded 10 May 2005 to 128.111.239.128. Redistribution subject to AIP license or copyright, see http://apl.aip.org/apl/copyright.jsp

TABLE I. Sputtering conditions.

| Target (3 in.) | Zr | Pt | BST |
|---|---|---|---|
| Power | 20 W (dc) | 33 W (dc) | 150 W (rf) |
| $Ar/O_2$ (sccm) | 100/0 | 100/0 | 90/10 |
| Substrate temperature | 23 °C | 600 °C | 700 °C |
| Gas pressure (mTorr) | 25 | 25 | 35 |

beam evaporation. The Au/Pt/BST/Pt capacitors were characterized using an Agilent 4294A variable frequency (40–110 MHz) impedance analyzer. The measured series resistances for shorted 30 $\mu$m by 50 $\mu$m capacitors with 20 $\mu$m spacing ranged from 310–340 m$\Omega$. A Keithley 540 CV Analyzer was used along with an MMR temperature probe station to measure capacitance over a 100–500 K temperature range at 1 MHz with a 500 mV oscillating electric field.

Stress $\sigma$ in polycrystalline sputtered films results from both an intrinsic $\sigma_{\mathrm{intrinsic}}$ and temperature-dependent component $\sigma_{\mathrm{thermal}}$:

$$\sigma_{\mathrm{film}}=\sigma_{\mathrm{intrinsic}}+\sigma_{\mathrm{thermal}}(T). \quad (1)$$

Various reasons exist for the development of intrinsic stress, including capillary pressure and grain coalescence, but the thermal contribution is due to the difference in thermal expansion coefficient between the film and the underlying substrate[7,8]

$$\sigma_{\mathrm{thermal}}=\int_{T1}^{T2}\frac{(\alpha_{\mathrm{film}}-\alpha_{\mathrm{substrate}})E_{\mathrm{film}}}{1-\nu_{\mathrm{film}}}dT, \quad (2)$$

$$\varepsilon_{\mathrm{thermal}}=\int_{T1}^{T2}(\alpha_{\mathrm{film}}-\alpha_{\mathrm{substrate}})dT, \quad (3)$$

where $E$, $\alpha$, and $\nu$ represent the elastic modulus, thermal expansion coefficient, and Poisson's ratio, respectively. It has been experimentally shown by Shaw *et al.* that stress is partly responsible for reducing the dielectric constant in BST thin films.[9] Pertsev *et al.* have shown that stress can shift the Curie–Weiss temperatures and therefore suppress the ferroelectric phase in thin films.[10] For (001) oriented fully relaxed epitaxial films, Pertsev *et al.* predicted that when the thermal expansion coefficient ($\alpha$) of the film is larger than the substrate, the renormalized Curie–Weiss temperature of the film ($\theta^*$) is lower than that of the free crystal ($\theta$) and the renormalized Curie–Weiss constant of the film ($C^*$) is larger than that of the free crystal ($C$).[10] Equations (4) and (5) detail the shift in Curie–Weiss constant and temperature as a function of electrostrictive tensor ($Q_{ij}$), elastic constant ($s_{ij}$), growth temperature ($T_g$), and misfit/growth strain $S_m(T_g)$ as given by Pertsev *et al.*[10] For a fully relaxed film at the growth temperature, $S_m(T_g)=0$

$$C^*=\frac{C}{1-4\varepsilon_0 C\frac{Q_{12}}{(s_{11}+s_{12})}(\alpha_{\mathrm{substrate}}-\alpha_{\mathrm{film}})}, \quad (4)$$

$$\theta^*=\frac{\theta+4\varepsilon_0 C\frac{Q_{12}}{(s_{11}+s_{12})}[S_m(T_g)-(\alpha_{\mathrm{substrate}}-\alpha_{\mathrm{film}})T_g]}{1-4\varepsilon_0 C\frac{Q_{12}}{(s_{11}+s_{12})}(\alpha_{\mathrm{substrate}}-\alpha_{\mathrm{film}})}. \quad (5)$$

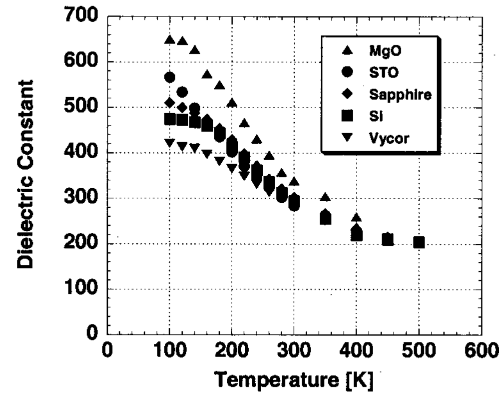


FIG. 1. Dielectric constant as a function of temperature for BST/Pt/substrate structures.

To understand the impact of the growth substrate, mainly the thermal expansion characteristics of the substrate on the dielectric permittivity of the deposited thin film, a direct comparison was made between the films on the platinized substrates (magnesium oxide, sapphire, silicon, strontium titanate, and vycor). Each substrate had a similar growth surface, (111) textured polycrystalline Pt on amorphous $SiO_2$, for the deposited BST film. Figure 1 shows the zero-bias dielectric constant as a function of temperature for the five samples, and Fig. 2 shows the dielectric constant as a function of applied voltage at 100 K. For bulk (Ba,Sr)$TiO_3$ ceramics, the Curie temperature linearly decreases from 120 °C for pure $BaTiO_3$ by 3.4 °C per mole percent of strontium.[11] Thus, we predict a bulk Curie temperature of ~134.75 K (−138.25 °C) for the $Ba_{0.24}Sr_{0.76}Ti_{0.96}O_3$ films. Both Figs. 1 and 2 clearly show a reduction in the dielectric constant for growth on substrates with smaller thermal expansion coefficients. Table II summarizes the thermal expansion, strain, and stress data for the substrates investigated.[12–15] To calculate the thermal stress in the films the elastic modulus and Poisson's ratio were estimated from bulk values at E ~200 GPa and $\nu$~0.23.[16] The thermal strain was calculated at 25 °C and 700 °C due to the lack of accurate thermal expansion data at low temperatures. The thermal mismatch between the BST film and strontium titanate substrate was

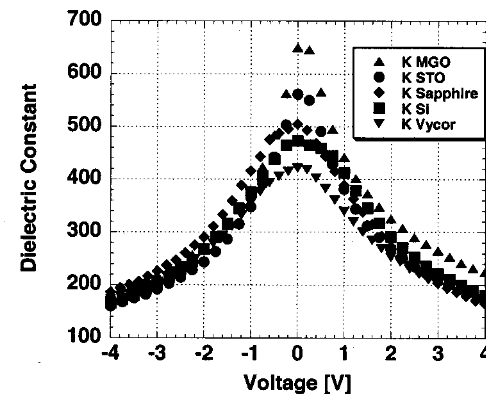


FIG. 2. Dielectric constant vs applied voltage at 100 K for BST/Pt/substrate structures.

Downloaded 10 May 2005 to 128.111.239.128. Redistribution subject to AIP license or copyright, see http://apl.aip.org/apl/copyright.jsp

TABLE II. Thermal expansion coefficients and calculated thermal strain and stress.

| Material | $\alpha$(25/700 °C) $10^{-6}$ °C | $\varepsilon_{\text{Thermal}}$ (%) | $\sigma_{\text{Thermal}}$ (GPa) |
|---|---|---|---|
| BST film (24/76) | 7.8/11 | | |
| MgO | 11.15/16.28 | −0.36 | −0.94 |
| Sapphire | 6/8.7 | 0.15 | 0.38 |
| Si | 2.618/4.4 | 0.44 | 1.16 |
| STO | 7.8/11 | 0 | 0 |
| Vycor | *0.75-1*[15] | ~0.68 | 1.77 |

set to zero because of the minimal difference between their expansion coefficients and their similar behavior at elevated temperatures. The film grown on the substrate with the largest expansion coefficient, magnesium oxide, had the highest dielectric constant compared to the smaller dielectric constants measured on the silicon and vycor substrates.

We have attributed the reduction in dielectric permittivity for films grown on substrates with lower thermal expansion coefficients to the larger tensile strain and larger reduction in the Curie–Weiss temperature. Linear extrapolation from the inverse susceptibility as a function of temperature determined the Curie–Weiss temperature ($\theta^*$) and constant ($C^*$) for the films. This is in agreement with the trends predicted by Pertsev *et al.* with Eqs. (4) and (5) that are plotted in Fig. 3.[10] The materials constants involved in Eqs. (4) and (5) include: $C=1.01\times10^5$ K, $Q_{12}=-0.015$ m$^4/C^2$, $T_g=700$ K, and $s_{11}+s_{12}=3.49\times10^{-12}$ Pa$^{-1}$.[16] Discrepancies

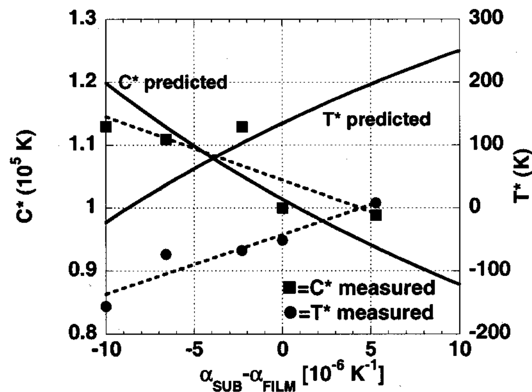


FIG. 3. Experimentally determined and predicted (solid lines) renormalized Curie–Weiss constant and ($C^*$) and Curie–Weiss temperature ($\theta^*$).

between the experimental results and the behavior predicted by Pertsev *et al.* are likely due to the weak texture in our films whereas Pertsev *et al.*'s model was developed for (001) oriented films.

In summary, by using a Pt growth surface on an amorphous $SiO_2$ interlayer and varying the substrate, the film–substrate thermal mismatch could be changed. Similar to other studies, our data clearly demonstrates that tensile strain reduces the dielectric permittivity of polycrystalline BST thin films. Future studies should investigate pure $SrTiO_3$ and $BaTiO_3$ films to determine the influence of thermal strain on their dielectric properties. Film orientation and grain size analysis will be studied in our future work.

This research has been supported by DARPA through the Frequency Agile Materials for Electronics Program (FAME) under Award No. DABT63-98-1-0006. Sputtering system fabrication was supported by the Army Research Office (ARO) through DURIP equipment Award No. DAAD19-99-1-0060. This work made use of the MRL Central Facilities supported by the National Science Foundation under Award No. DMR 96-32716. RBS analysis was done by the Ion Beam Facility of CCMR, Cornell University supported through NSF Grant DMR-9632275. The authors thank Professor S. Stemmer for many useful conversations and for alerting us to Ref. 9.

[1] J. S. Speck and W. Pompe, J. Appl. Phys. **76**, 466 (1994).
[2] J. S. Speck, A. Seifert, W. Pompe, and R. Ramesh, J. Appl. Phys. **76**, 477 (1999).
[3] A. E. Romanov, W. Pompe, and J. S. Speck, J. Appl. Phys. **79**, 4037 (1996).
[4] W. Pompe, X. Gong, Z. Suo, and J. S. Speck, J. Appl. Phys. **74**, 6012 (1993).
[5] N. A. Pertsev, A. G. Zembilgotov, and A. K. Tagantsev, Phys. Rev. Lett. **80**, 1988 (1998).
[6] S. K. Streiffer, C. Basceri, C. B. Parker, S. E. Lash, and A. I. Kingon, J. Appl. Phys. **86**, 4565 (1999).
[7] M. Ohring, *The Materials Science of Thin Films* (Academic, New York, 1991).
[8] R. W. Hoffman, Thin Solid Films **34**, 185 (1976).
[9] T. M. Shaw, Z. Suo, M. Huang, E. Liniger, R. B. Laibowitz, and J. D. Baniecki, Appl. Phys. Lett. **75**, 2129 (1999).
[10] N. A. Pertsev, A. G. Zembilgotov, S. Hoffman, R. Waser, and A. K. Tagantsev, J. Appl. Phys. **85**, 1698 (1999).
[11] S. Ezhilvalavan and T.-Y. Tseng, Mater. Chem. Phys. **65**, 227 (2000).
[12] D. Taylor, J. Br. Ceram. Soc. **84**, 181 (1985).
[13] V. Srikant, E. J. Tarsa, D. R. Clarke, and J. S. Speck, J. Appl. Phys. **77**, 1517 (1995).
[14] C. A. Swenson, J. Phys. Chem. Ref. Data **12**, 179 (1983).
[15] Thermal expansion data for Vycor glass only available from 0 °C–300 °C by the manufacturer: Precision Glass and Optics, Santa Ana, California.
[16] Landolt–Börnstein, *Numerical Data and Functional Relationships in Science and Technology*, New Series Vol. III/29a (Springer, Berlin, 1992).

Downloaded 10 May 2005 to 128.111.239.128. Redistribution subject to AIP license or copyright, see http://apl.aip.org/apl/copyright.jsp